BioOne DIGITAL LIBRARY

BURLY GAITS: CENTERS OF MASS, STABILITY, AND THE TRACKWAYS OF SAUROPOD DINOSAURS

Author: HENDERSON, DONALD M.

Source: Journal of Vertebrate Paleontology, 26(4) : 907-921

Published By: The Society of Vertebrate Paleontology

URL: https://doi.org/10.1671/0272-4634(2006)26[907:BGCOMS]2.0.CO;2

The BioOne Digital Library (https://bioone.org/) provides worldwide distribution for more than 580 journals and eBooks from BioOne's community of over 150 nonprofit societies, research institutions, and university presses in the biological, ecological, and environmental sciences. The BioOne Digital Library encompasses the flagship aggregation BioOne Complete (https://bioone.org/subscribe), the BioOne Complete Archive (https://bioone.org/archive), and the BioOne eBooks program offerings ESA eBook Collection (https://bioone.org/esa-ebooks) and CSIRO Publishing BioSelect Collection (https://bioone.org/csiro-ebooks).

Your use of this PDF, the BioOne Digital Library, and all posted and associated content indicates your acceptance of BioOne's Terms of Use, available at www.bioone.org/terms-of-use.

Usage of BioOne Digital Library content is strictly limited to personal, educational, and non-commmercial use. Commercial inquiries or rights and permissions requests should be directed to the individual publisher as copyright holder.

BioOne is an innovative nonprofit that sees sustainable scholarly publishing as an inherently collaborative enterprise connecting authors, nonprofit publishers, academic institutions, research libraries, and research funders in the common goal of maximizing access to critical research.

Downloaded From: https://complete.bioone.org/journals/Journal-of-Vertebrate-Paleontology on 21 Mar 2025
Terms of Use: https://complete.bioone.org/terms-of-use

Journal of Vertebrate Paleontology 26(4):907–921, December 2006
© 2006 by the Society of Vertebrate Paleontology

BURLY GAITS: CENTERS OF MASS, STABILITY, AND THE TRACKWAYS OF SAUROPOD DINOSAURS

DONALD M. HENDERSON*
Vertebrate Morphology and Palaeontology Research Group, Department of Biological Sciences, University of Calgary, Calgary, Alberta T2N 1N4, Canada; dmhender@ucalgary.ca

ABSTRACT—The narrow- and wide-gauge trackways attributed to sauropod dinosaurs are hypothesized to be a consequence of the relative positions of their centers of mass. This hypothesis was tested using three-dimensional, trackway-producing computer models of two sauropods and studies of Asian elephants. Centers of mass of sauropod models were computed using density distributions that reflect the high degree of pneumatization of the skeletons and air sacs within the body. A close correspondence was found between the relative areas of hand and foot prints in different trackways and the relative fractions of the body weight borne by the forefeet and hindfeet in the different types of sauropods inferred to have made the trackways. Experimental studies of Asian elephants corroborated the close correspondence between relative areas of the hindfeet and forefeet and body weight distribution. Replicating actual sauropod trackways with the walking models enabled testing of proposed gaits for a sauropod model. *Brachiosaurus brancai*, with its more centrally positioned center of mass, was stable and possessed a wide safety margin only when replicating a wide trackway. Conversely, *Diplodocus carnegii*, with a more posteriorly placed center of mass, was most stable when replicating a narrow trackway. A trend for large sauropods (>12 tons), independent of clade, to have more anteriorly positioned centers of mass was identified, and it is proposed that all large sauropods were restricted to producing wide-gauge trackways for stability reasons. The primitive gait state for Sauropodomorpha was determined to be one that produced narrow-gauge trackways.

INTRODUCTION

Sauropod dinosaurs are the largest terrestrial animals known to have existed, with typical body masses in the range of 10–20 tons (Pecksis, 1994), although for some extremely large forms, e.g., *Argentinosaurus*, estimates as high as 90 tons have been proposed (Paul, 1997). Preserved trackways left by these dinosaurs are relatively common (Farlow, 1992; Lockley et al., 1994), and allow inferences about the biology and behavior of these animals that is not obtainable from skeletal remains. Sauropod trackways can be broadly classed as either 'wide-gauge,' with hindfoot impressions relatively far from the midline, or 'narrow-gauge,' with the hind prints close to or overlapping the midline of the trackway (Farlow et al., 1989; Lockley et al., 1994) (Fig. 1A). Narrow-gauge sauropod trackways dominated for most of the Jurassic, while wide-gauge trackways predominated during the Cretaceous, but during a period spanning the latest Jurassic and earliest Cretaceous, both types had roughly similar abundances (Wilson and Carrano, 1999). It has been proposed that the narrow-gauge trackways were made by animals whose limbs were inclined medially, while the wide-gauge trackways were made by animals whose limbs were held vertically (Farlow, 1992). A detailed analysis of the hindlimbs and pelvic girdles of titanosaurs strongly suggests that these Cretaceous sauropods were osteologically capable of making the wide-gauge trackway (Wilson and Carrano, 1999). However, a biomechanical/functional explanation for the two different 'gauges' of trackway has remained elusive (Farlow, 1992).

When considering the body weight borne by the limbs of sauropods, or any other quadrupedal tetrapod, it is instructive to view the body as a simply supported beam, with the forelimb and hindlimb pairs acting as the columnar supports under the beam (Alexander, 1985). The fraction of the beam's weight borne by each of its supporting columns is equal to 1 minus each column's proportional distance from the center of mass (CM) of the beam (Halliday et al., 1993). For a centrally placed load, the weight borne by each of the supports will be equal (Fig. 2A), but an off-center load will result in the column closest to the load bearing a greater fraction of the weight than that carried by the column furthest from the load (Fig. 2B). The 1000 N load in Figure 2B is located 25% of the distance between the ends of the beam, so the support at the left-hand side bears 1–25%, or 75% (750 N) of the load. If the cross-sectional areas of the supporting columns are the same, the different fractions of the load carried by each column will result in different stresses acting at the base of each column. However, if the bases of the two columns can be adjusted so that the basal area of the more heavily loaded column increased, while that of the lightly loaded one reduced, the stresses can be made equal (Fig. 2B). This relationship between the loads experienced by columns, their cross-sectional areas, and the associated stresses, are relevant to the mechanics of the limbs and feet of tetrapods.

The plantar area of a human foot is a good indicator of body mass, and the stress experienced by the feet of differently sized individuals is relatively constant (Robinson and Frederick, 1989). Narrow-gauge sauropod trackways are associated with relatively small handprints, while wide-gauge trackways have relatively large handprints (Lockley et al., 1994) (Fig. 1B). It is hypothesized that these differences in manus print sizes indicate different relative fractions of body weight being carried by the forelimbs of narrow- and wide-gauge sauropod trackmakers—a result of different longitudinal positions of the CM in different sauropod taxa. Furthermore, the differing positions of the CM relative to the shoulders, hips, hands, and feet are predicted to have constrained how these animals walked and balanced.

To test the hypothesized correlations between relative manus and pes print areas, the position of the CM, and the generation of narrow- and wide-gauge trackways, dynamic models of the limbs and bodies of two different sauropods were generated. With computed values for the positions of the CM of the models, the effect of this parameter on potential gaits of sauropods was

* Present address: Royal Tyrrell Museum of Palaeontology, PO Box 7500, Drumheller, Alberta T0J 0Y0, Canada.

Downloaded From: https://complete.bioone.org/journals/Journal-of-Vertebrate-Paleontology on 21 Mar 2025
Terms of Use: https://complete.bioone.org/terms-of-use

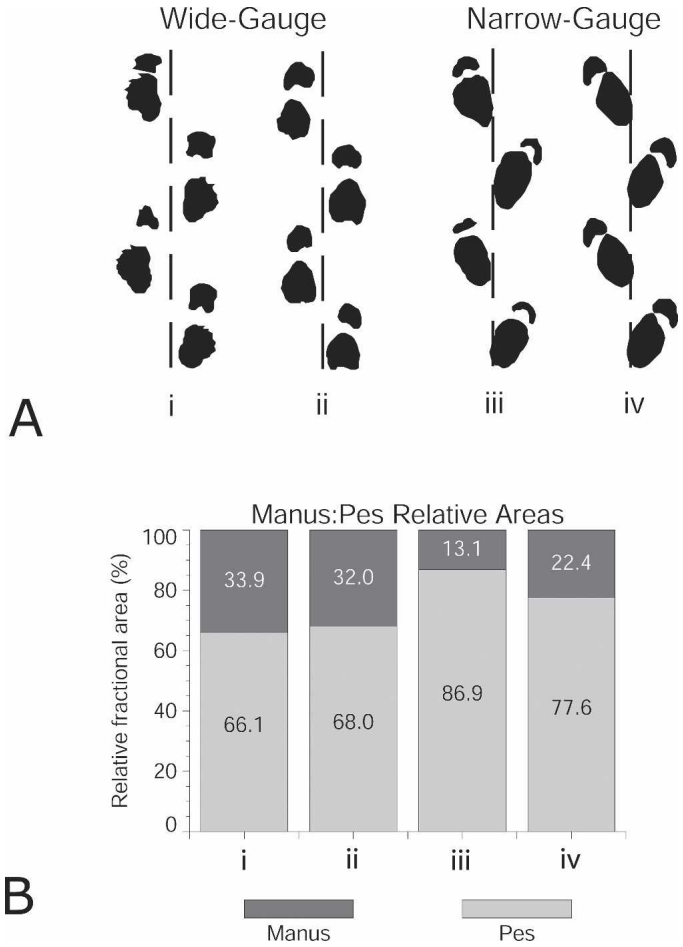

FIGURE 1. **A**, four examples of sauropod trackways demonstrating wide- and narrow-gauge trackways. Adapted from Thulborn (1990:fig. 6.15). Sources: (i) Farlow (1987), (ii) Pittman (1984), (iii) Ishigaki (1985), (iv) Dutuit and Ouazzou (1980). **B**, mean manus and pes print areas computed for the trackways of **A**, and plotted as bar graphs with the areas expressed as percentages of the combined area of a single handprint + footprint pair.

then assessed. The hypothesis that the manus and pes areas reflect the fractions of body weight that the respective limbs bear, and that computer models of tetrapods can be used to accurately determine the CM of the body, was checked with experiments using three large Asian elephant cows.

MATERIALS AND METHODS

Determining the Distribution of Body Weight in Elephants

Three Asian elephant cows (*Elephas maximas*) held at the Calgary Zoo (Calgary, Alberta, Canada) were carefully weighed to determine the fractions of their body weight carried on their forelimbs and hindlimbs: 'Ronnie' (Collection No. 103424), 'Kamala' (Collection No. 100731), and 'Swarna' (Collection No. 100730). A bull Asian elephant held at the Zoo, although much larger than the cows, was too aggressive to be used in the experiments. Body weight was ascertained using a set of large scales normally used to weigh trucks. To obtain total body weight (to act as a check on the sum of the forelimb and hindlimb weights) the animals were first weighed using the zoo's normal procedure of having the animals stand with their forefeet on one weighing pad and their hindfeet on the other pad (Fig. 3A). To record the weight acting on the forelimbs, the weighing pads were each put under one of the forefeet, while the hindfeet were placed on wooden blocks, as the animals were uneasy and unfamiliar with only having the weighing pads under one set of feet (Fig. 3B). This latter process was repeated, but with the weighing pads under the hindfeet, and the blocks under the forefeet.

Determining Elephant Footprint Areas

Within their indoor winter enclosure, the elephants normally walk on a thick, smooth rubber substrate. The elephants were guided through a shallow puddle of water and then led around their enclosure at a walking pace to leave wet footprints. The perimeters of these footprints were quickly outlined in chalk as soon as they were made and then photographed. The photographs were then scanned and the outlines of the footprints were digitized and their areas computed using a method developed for estimating skull orbital area (Henderson, 2002).

Matching Wide- and Narrow-Gauge Sauropod Trackways to Trackmakers

The well-documented, Early Cretaceous ichnogenus *Brontopodus birdi* (Farlow et al., 1989) was chosen as the standard for a wide-gauge trackway (Fig. 1A). It has been proposed that the poorly known Early Cretaceous brachiosaurid *Pleurocoelus* was

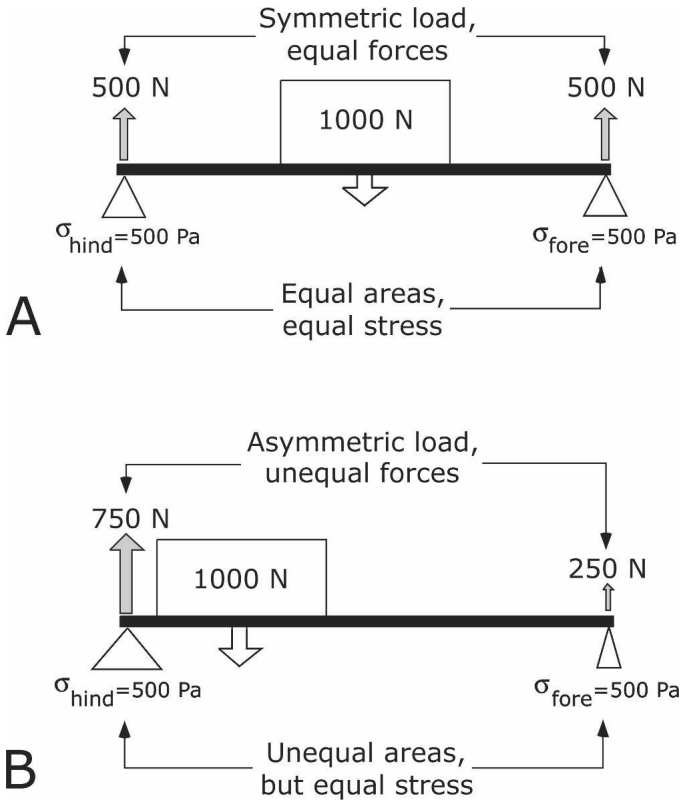

FIGURE 2. Schematic views of a loaded, simply supported beam demonstrating the different fractions of the load borne by the supporting end points when the load is positioned at different points along the beam. **A**, for a centrally placed load the weight experienced by both supports is the same, and with similar cross-sectional areas for the two supports, the stresses acting at their bases are the same. **B**, for an asymmetrically loaded beam the supporting element closest to the load will carry most of the weight, while the opposite support experiences a reduced load. Only by increasing the area of more heavily loaded support, and reducing the area of the lightly loaded support, will the stresses in the supports equal those observed in the symmetric loading example. A similar situation is interpreted to be occurring in sauropods as indicated by the marked differences in the sizes of their handprints and footprints.

Downloaded From: https://complete.bioone.org/journals/Journal-of-Vertebrate-Paleontology on 21 Mar 2025
Terms of Use: https://complete.bioone.org/terms-of-use

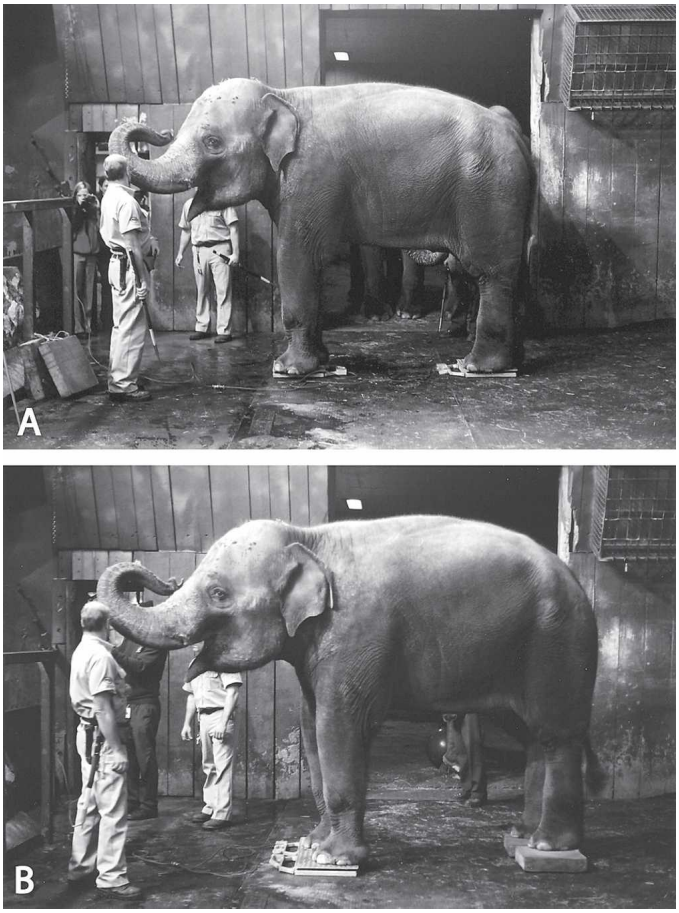

FIGURE 3. Controlled weighing of the Calgary Zoo elephant cow Ronnie (*Elephas maximas*) to determine the fractions of body weight carried by her forelimbs and hindlimbs. **A**, full weight determination with the weighing scales positions under the forefeet and hindfeet. **B**, forelimb loading determination with both scales under the forefeet, and 'dummy' blocks under the hindfeet. See Table 1 for summaries of the limb loadings and foot areas.

the maker of this trackway (Farlow et al., 1989; Langston, 1974). The recent discovery of the large, but incompletely preserved, brachiosaurid, *Sauroposeidon proteles* from the Early Cretaceous of Oklahoma, provides another potential *Brontopodus* trackway maker (Wedel and Cifelli, 2005). However, the more completely known Late Jurassic brachiosaurid *Brachiosaurus brancai* was chosen as the model for attempting to replicate *Brontopodus birdi*. *Diplodocus carnegii* is known from several skeletons, and was chosen as the potential producer of a narrow-gauge trackway because both diplodocids and narrow-gauge trackways were common during the Late Jurassic (McIntosh et al., 1997; Wilson and Carrano, 1999). An unnamed Upper Jurassic, narrow-gauge trackway from Morocco (Ishigaki, 1985) (Fig. 1C) was deemed the most appropriate to represent that made by a diplodocid, because the relative proportions of its handprint and footprint areas—large pes, very small manus—coincided with a preliminary estimation of a more posterior position for the CM of *Diplodocus* (Alexander, 1985; Henderson, 1999). Additionally, the arcuate forms of the manus prints of the Moroccan trackway are similar to what could have been produced by the tightly bundled, columnar metacarpals of a diplodocid (Thulborn, 1990). Although the large diplodocid *Torneiria* is known from Africa in the Late Jurassic, it was not used in this study because its skeleton is not as complete as that of *Diplodocus*.

Computational Body Mesh Definitions

Elephant—A computational mesh representation of the axial body and limbs of the largest *Elephas* cow at the Calgary Zoo (Kamala) (Fig. 4A) was derived from lateral view photographs of the animal in combination with posterior views of Asian elephants from the photographs in Muybridge (1887:pl. 111). To make the model as realistic as possible, a lung volume was included in the calculations of mass and center of mass. A scaling relationship for lung volume versus body mass for mammals (lung volume in liters $= 0.0535 \cdot M_{body}^{1.06}$: Stahl, 1967), predicts the lung volume in this 3290-kg animal to be 286.1 L. It was assumed that the mean tissue density for the entire elephant was 1000 g/L, and the space representing the lungs was set as a hollow cavity of volume 286.1 L placed in the anterodorsal region of the thoracic cavity below the level of the spinal column (medium gray region in Fig. 4A).

Sauropods—The dinosaur models were initially based on published restorations that provided both lateral and dorsal views (*Brachiosaurus*: Paul, 1987; *Diplodocus*: Paul, 1997), but the axial body shapes were later modified with the addition of new data (Fig. 4B, C). With original measurements collected from the axial skeleton of *Diplodocus carnegii* (Carnegie Museum of Natural History [CM] 94), it was found that the trunk region of the Paul (1997) restoration had to be lengthened to accommodate all of the vertebrae. The first version of the Paul-based *Brachiosaurus* model produced manual tracks that were consistently obscured by pedal ones, completely unlike the pattern seen in *Brontopodus birdi*, so the body was lengthened by 70 cm to displace the manus prints forward. This change had the added bonus of making the gleno-acetabular (GA) length of the digital *Brachiosaurus* model consistent with that estimated from a stereophotogrammetrically derived plot of the skeletal mount at the Museum of Natural History, Berlin, Germany (Gunga et al., 1995). The neck of the *Brachiosaurus* model was also inclined to a more forward leaning (less vertical) posture than it was in the original restoration.

Brachiosaurus is a macronarian sauropod (Upchurch et al., 2004), and in the Paul (1997) illustration of the Humboldt *Brachiosaurus* mount the tail is rather short, with a ratio of tail length (measured from the acetabulum to the tip of the tail) to GA length of just 2.0. A comparison of the tail lengths relative to GA lengths in other relatively complete macronarian sauropods revealed a different ratio value. Using published restorations of three macronarians with complete post-cervical regions (Paul, 1997), the following ratios were found: *Camarasaurus*, 2.88; *Jobaria*, 2.40; *Opisthocoelicaudia*, 2.60; with a mean of 2.63. The tail and trunk length ratios in two other exceptionally long-necked sauropods—the relatively complete basal eusauropods *Omeisaurus* and *Mamenchisaurus* (Upchurch et al., 2004)—showed that they had ratios of 2.62 and 2.5, respectively, again highlighting the undersized tail of the Humboldt mount. The Berlin *Brachiosaurus* is a composite of the remains of several individuals (Christian and Heinrich, 1998), with the presacral axial skeleton and the tail of this mount being from different animals (Gunga et al., 1995). This fact, and the higher tail:trunk ratio seen in macronarians and other sauropods, led to the tail of *Brachiosaurus* model being conservatively extended so that its length was equal to 2.5 times the length of the trunk.

Assigning Densities to Sauropod Body Regions

A theoretical study of breathing mechanics in sauropods suggests that they would have required a breathing system similar to that of birds with air sacs (Daniels and Pratt, 1992), and the system of abdominal and thoracic air sacs in birds occupies 15% of the volume of the trunk (Proctor and Lynch, 1993). Using birds as the starting point, sets of paired, triaxial ellipsoids rep-

Downloaded From: https://complete.bioone.org/journals/Journal-of-Vertebrate-Paleontology on 21 Mar 2025
Terms of Use: https://complete.bioone.org/terms-of-use

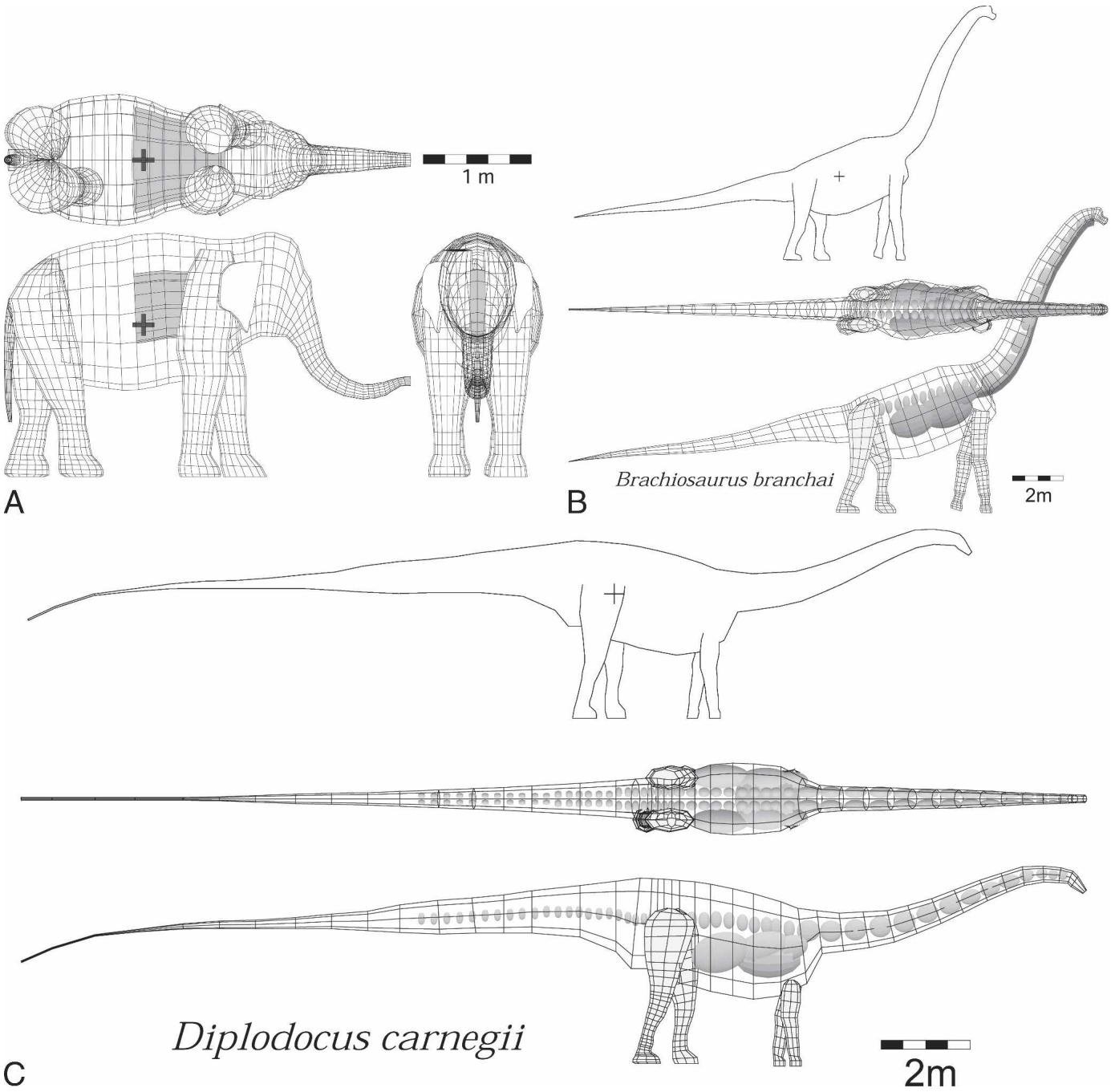

FIGURE 4. **A**, digital model of the largest of the three Asian elephants (*Elephas maximas*) used in this study (Kamala, Calgary Zoo, Calgary, Alberta, Canada). The light gray region in the chest area represents the lung volume, which was treated as an air-filled cavity. The rest of the body was modeled as being solid with a density equal to that of water (1000 g/L). The black '+' indicates the computed center of mass (CM) of the body, which gives forelimb and hindlimb loadings within 2% of those observed for the living form. Digital models of **B**, *Brachiosaurus branchai* and **C**, *Diplodocus carnegii* demonstrating the volumes and distributions of the internal air-sacs, lungs, and trachae. The two-dimensional silhouettes illustrate the computed CMs that result from the mesh geometries and density distributions. See Table 2 for summaries of the regional masses and densities of these models.

resenting thoracic and abdominal (posterior and anterior) air sacs were generated for the sauropod models, and their dimensions adjusted until their combined volumes equaled 15% of the trunk volume (Fig. 4B, C). From an allometric scaling relationship between body mass and lung volumes in birds ($0.0296 \cdot \text{Mass}_{\text{body}}^{0.94}$: Schmidt-Nielsen, 1984), the lung volumes for *Brachiosaurus* (25.9 t) and *Diplodocus* (11.4 t) are 392 L and 205 L, respectively, and these volumes represent 2.0% and 2.5%, respectively, of the total trunk volumes. It is poor practice to extrapolate an allometric relationship beyond the original range of the data used to define it. However, it was thought that use of the bird lung to body mass scaling function was the only objective way to make preliminary estimates for the lung volumes in sauropods. Combining lungs, abdominal and thoracic air sacs, and dorsal axial air sacs (Wedel, 2003a), and treating them all as air-filled cavities, gives the trunk region a mean density of ap-

Downloaded From: https://complete.bioone.org/journals/Journal-of-Vertebrate-Paleontology on 21 Mar 2025
Terms of Use: https://complete.bioone.org/terms-of-use

proximately 800 g/L, which was used for both the *Brachiosaurus* and *Diplodocus* models. The extreme reduction in the amount of bone present in sauropod cervical vertebrae (Wedel, 2004), and evidence for an extensive system of air sacs and pneumatization along the cervical series (Wedel, 2003a, b) indicates very low neck densities. Hypothetical cervical air sacs were generated for both *Brachiosaurus* and *Diplodocus* with the assumption that they would lie within the large, lateral pleurocoels of the vertebrae and extend laterally as far as the cervical ribs (Fig. 4B, C). The volumes of cervical air sacs represent 47.7% and 37.3%, respectively, of the total volumes of the head and neck in *Brachiosaurus* and *Diplodocus*. Additionally, the extreme internal bone reduction in the cervical vertebrae of the very large, Early Cretaceous brachiosaurid *Sauroposeidon* (Wedel et al., 2000; Wedel, 2004), and other sauropods, strongly implies very low neck densities in these animals. Bramwell and Whitfield (1974) found that the density of a goose neck was 300 g/L, and this value was used for the densities of the heads and necks in both sauropod models. The presence of a wide trachea (Daniels and Pratt, 1992) would also contribute to a low neck density. The densities of the tails and limbs of both models were assigned the densities of water at 1000 g/L. The sauropod density distributions developed here are refinements of earlier models (Henderson, 2004).

Limb Motions

The limbs of the sauropod models were represented as a series of connected nodes in three-dimensional space that represent joint positions (Fig. 5), and at each joint position the orientation of the axis of rotation of the joint was specified with a vector in three-dimensional space. For each model, the hindlimb was defined as a hip, knee, ankle, a single distal metatarsal joint that the pedal phalanges rotated about in unison, and a distal end to the pedal phalanges. The forelimb node set for each model consisted of shoulder, elbow, wrist, and a distal end to the metacarpals. However, the wrist joint was made immobile (see Results), which resulted in the forelimb having flexion/extension at just the elbow. This single hinge state differs from the hindlimb with its pair of distal hinges (knee and ankle). The details of the system of joints and their associated axes of rotation can be found in Henderson (in press).

With the limb joints represented as mathematical points it is possible to derive systems of partial differential equations that relate the positions of the joints to the angles between the bones. For a specified displacement of either a proximal or distal part of a limb in three-dimensional space, the system of differential equations is solved to determine what angular changes are to be applied to the joints to effect the required displacement. The details of the mathematical methods can be found in Henderson (in press).

With the very high mass estimates for sauropods, and the observation that very large extant animals move in such a way that large accelerations and bending stresses are minimized (McMahon, 1975; Biewener, 1989; Alexander, 1997), the sauropod models were limited to slow, lateral-sequence (Hildebrand, 1985) walking gaits. Only one limb of the model was in the swing phase at any time, and it would only lift off the substrate and begin to protract when the horizontal position of the CM was within a triangle of support defined by the three, stance-phase limbs (see below). In accordance with observations of elephant locomotion (Gambaryan, 1974), the models were additionally constrained so that there was no vertical displacement of the body at any time.

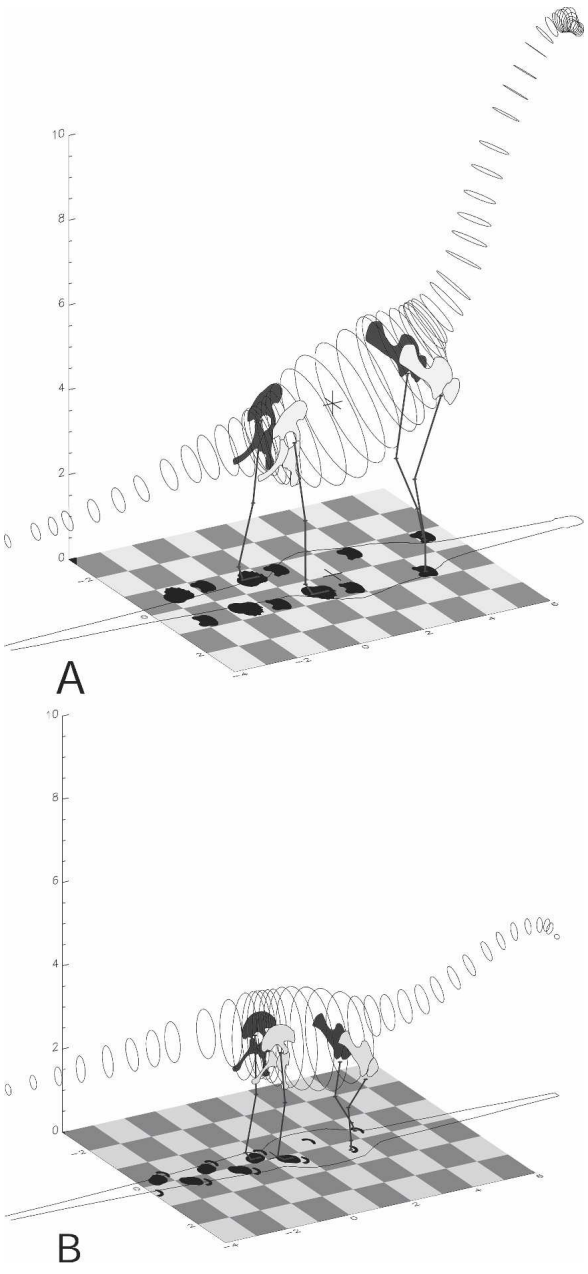

FIGURE 5. Posterolateral views of the three-dimensional walking, digital models of the sauropods and the trackway traces that are generated. The three-dimensional, black '+' denoting CM of the *Brachiosaurus* (**A**) is visible in the center of its trunk, but the CM of *Diplodocus* (**B**) is hidden behind the right ilium. The CM is also projected onto the floor, along with a frontal outline of the axial body. Both pairs of limbs of *Brachiosaurus* are vertical, while those of *Diplodocus* are medially inclined. The more flexed forelimbs of the *Diplodocus* model were required to allow the forelimbs to have the same stride length as the much longer hindlimbs. Limb girdle shapes and limb dimension sources: *Brachiosaurus* (Paul, 1987); *Diplodocus* (Hatcher, 1901) (Carnegie Museum of Natural History [CM] 94). Body shapes adapted from the following sources: *Brachiosaurus* (Paul, 1987); *Diplodocus* (Paul, 1997). Floor tile dimensions are 1 m by 1 m.

Stability Triangle

A basic rule for any quadrupedal terrestrial animal is that it takes at least three points of contact with the substrate to maintain the body in a state of stable equilibrium. A further requirement is that the horizontal position of the CM of the animal lies within a triangular region whose vertices are defined by the three points of contact (Gray, 1968). If the CM lies outside this 'stability triangle,' the animal will tip over. This constraint of maintaining the CM within the stability triangle was applied at all stages of a walk cycle by a combination of visual inspection of the

Downloaded From: https://complete.bioone.org/journals/Journal-of-Vertebrate-Paleontology on 21 Mar 2025
Terms of Use: https://complete.bioone.org/terms-of-use

CM during the animation of a gait, and by determining the loading on the limbs.

Calculation of the fractions of body weight borne by the limbs was done under the assumption that at each stage of a step cycle the net forces and torques acting on the body would produce no vertical or lateral motions, and the body would not rotate about any axes (Gray, 1968). For example, with the left arm in swing phase (not contacting the substrate), and the two hindfeet and the right hand in contact with the substrate, the combined loads borne by the two hindlimbs and the right arm must equal the animal's weight. Because our interest is in the relative fractions of the total weight carried by each of the stance phase limbs, the vertical force balance equation is expressed in terms of percentages of total body weight acting on each limb:

$$\sum F_y = F_{RightFoot} + F_{LeftFoot} + F_{RightHand} = 100\% \quad (1)$$

where $\boldsymbol{F}_{RightFoot}$, $\boldsymbol{F}_{LeftFoot}$, and $\boldsymbol{F}_{RightHand}$ are relative forces acting through the right and left feet and the right hand, and together these forces represent 100% of the body weight. $\boldsymbol{F}_y$ indicates that we are only concerned with forces acting in the vertical (Y-axis) direction. The equations for no net turning forces about the two horizontal axes, X (anteroposterior) and Z (mediolateral), are:

$$\sum \tau_x = F_{RightFoot} \cdot d^z_{RF} + F_{LeftFoot} \cdot d^z_{LF} + F_{Righthand} \cdot d^z_{RH} = 0 \quad (2)$$

$$\sum \tau_z = F_{RightFoot} \cdot d^x_{RF} + F_{LeftFoot} \cdot d^x_{LF} + F_{Righthand} \cdot d^x_{RH} = 0 \quad (3)$$

where $\boldsymbol{d}^x_{RF}$ and $\boldsymbol{d}^z_{RF}$ are the anteroposterior and mediolateral distances, respectively, of the right foot from the CM, with similar symbols used for the distances associated with the left foot and right hand. At each stage of the step cycle this system of equations {(1), (2), (3)} was solved to determine the fraction of body weight borne by each supporting limb. The lack of vertical motion in the models implies that there are no vertical accelerations acting on the body other than that associated with gravity, and when combined with the slow gait, it permits the forces acting on the limbs to be approximated as being directly proportional to the body weight. Equations (1), (2), and (3) are set up such that the forces computed for any limb will always be positive when the CM lies within the triangle of stability. If the CM lies outside of the triangle one or more of the computed the forces will be negative, and this will signal a limb + body configuration that is not in stable equilibrium. To obtain a stable model the gait angles and mediolateral displacements for each model were adjusted until all the limb load fractions were positive, although this was not always possible for some combinations of gaits with the models.

RESULTS

Elephant Body Mass Distribution and Relative Track Areas

Table 1 presents data on the weights of the Asian elephants. Two of the three sets of measurements (for Swarna and Kamala—the heaviest animals) demonstrate a close correlation between the relative areas of the forefoot and hindfoot impressions and the fractions of body weight that they carry. The two types of relative measurement for a given hand or foot—area and loading—are within 1% or 2% of each other, and support the hypothesis that foot structure and area reflect the forces that they must carry. This pattern breaks down with the smallest animal of the three (Ronnie). Although her forelimbs take the larger fraction of her body weight, with forefoot and hindfoot proportions very similar to those seen in the other two animals, her feet are more equal in size, with the result that the computed stress on the forefeet is roughly 50% greater than that for the hindfeet.

There are at least three possible explanations for this discrepancy. First, because Ronnie is not fully grown, the proportions of her feet may have not attained the final adult state. However, Ronnie's forefeet are still larger in area than her hindfeet, in keeping with what is seen in Swarna and Kamala. Second, during the weighings, the elephants would tend to lean to one side, or lean back (slouching) while standing on the scales. Any deviation from having perfectly vertical limbs would affect the loadings recorded by the weighing scales. It may be that some incidences of slouching in Ronnie went unobserved, and this affected the final results. Third, the foot pressure applied to the rubber substrate was not uniform, and tended to be greatest toward the centers of the feet and diminish toward the edges. The wet footprint impressions of Ronnie's pads may not have fully recorded the true proportions of her feet because she is the lightest of the three elephants.

Figure 4A shows the three-dimensional digital model of Kamala along with the CM position indicated by a black '+.' With the uniform body density of 1000 g/L (except for the region of the lung), and the lung volume derived from a general allometric scaling relationship for mammals, the mass of the computed model is 3088.7 kg (Table 2). The observed mass of Kamala was 3290 kg. The computed CM lies in front of the acetabulum at a point equal to 57.25% of the horizontal gleno-acetabular distance. The weighings of Kamala demonstrated that her CM was situated at a point 59.5% ahead of her acetabulum. This close correspondence between the observed and modeled CM positions clearly demonstrates that a three-dimensional digital model can adequately replicate a biomechanical aspect of an organism based on a carefully specified density and mass distribution.

Sauropod Body Mass, Its Distribution, and Relative Track Areas

Outline silhouettes in Figures 4B and 4C illustrate the computed CMs of the two sauropods (Table 2 presents the total masses, component masses, and the numerical values for the relative CM position in these two models). The CM of *Brachiosaurus* can be seen to lie almost centrally in the trunk, while that of *Diplodocus* lies immediately in front of the hips. Relative to

TABLE 1. Indian elephant cow (*Elephas maximas*) fore- and hindlimb loadings and foot print areas.

Name		Forelimb		Hindlimb	
Total mass		Actual quantity	Fraction	Actual quantity	Fraction
'Ronnie' 2,785 kg	Limb load (kg)	1,753.0	62.0%	1,073.0	38.0%
	Print area (m^2)	0.1432	53.2%	0.1261	46.8%
	Stress (kPa)	60.045		41.737	
'Swarna' 2,921 kg	Limb load (kg)	1,839.0	64.6%	1054.0	36.4%
	Print area (m^2)	0.1871	63.8%	0.1062	36.2%
	Stress (kPa)	48.211		48.681	
'Kamala' 3,290 kg	Limb load (kg)	1947.5	59.5%	1325.0	40.5%
	Print area (m^2)	0.1212	57.7%	0.0888	42.3%
	Stress (kPa)	78.816		73.188	

Downloaded From: https://complete.bioone.org/journals/Journal-of-Vertebrate-Paleontology on 21 Mar 2025
Terms of Use: https://complete.bioone.org/terms-of-use

TABLE 2. Linear dimensions of the two walking sauropod models, and details of the synthetic trackways produced by each model when using its preferred gait.

	Brachiosaurus brancai (wide-gauge)	*Diplodocus carnegii* (narrow-gauge)
Shoulder height (glenoid) (m)	4.00	1.67
Hip height (acetabulum) (m)	3.67	2.78
Hindlimb excursion angle	9°	8°
Gleno-acetabular distance (m)	4.65	2.75
Stride length (m)	2.32	1.57
Pace angulation (hind limb)	105°	137°
Relative position of CM[1]	37.4	11.5

[1]Expressed as a percentage of the gleno-acetabular distance in front of the hips.

the position of the acetabulum, the position of the CM can be conveniently expressed as percentages of the gleno-acetabular (GA) distance, and for *Brachiosaurus* and *Diplodocus* these fractions are 37.4% and 11.5%, respectively. These numbers imply that the hind feet of *Brachiosaurus* would, when averaged over a complete step cycle, carry 62.6% of the body, while in *Diplodocus* the hind limb carrying fraction would be 88.5%. For the wide-gauge *Brontopodus birdi* trackway (Fig. 1A(i)) the area ratio manus:pes is 33.9 to 66.1, while for the unnamed narrow-gauge trackway (Fig. 1A(iii)), the ratio is 13.1 to 86.9. In calculating the manual area of the *Brontopodus birdi* trackway only the undistorted horseshoe-shaped manus prints were used (right manual impressions) as these had the best correspondence to restored manus forms for macronarians (Bonnan, 2003). From these area ratios it can be seen that there is a reasonable correspondence between the relative areas of the manüs and pedes and the predicted fractions of body weight that they would bear, with the mismatch being 3.5% in the case of *Brachiosaurus* and 1.6% in *Diplodocus*. These minor mismatches do not negate initial assumptions that *Brontopodus birdi* was made by an animal similar to a *Brachiosaurus*, nor that the unnamed, narrow-gauge trackway was made by a sauropod with a body similar to *Diplodocus*.

Figure 5 presents three-dimensional views of the two sauropod walking models in posterolateral view in association with the wide- and narrow-gauge tracks generated by the limb and body motions of the models over the course of several step cycles. The synthetic track patterns are good facsimiles of the original fossil tracks (Fig. 1A,C). Characteristics of the trackways and their makers are summarized in Table 3.

To test the robustness of the inferences that the narrow- and wide-gauge trackways could have been made by sauropods like *Diplodocus* and *Brachiosaurus*, an analysis was carried out to see how well each model could replicate both kinds of trackways, and how stable each model was when doing so. To facilitate comparisons between the models, the *Brachiosaurus* and the *Diplodocus* models were both given a standard gait, with 4 of 16 frames allotted for the swing (protractive) phase of a limb and 12 of 16 frames allotted for the stance (retractive) phase. This resulted in the minimum duty factor possible for each limb (0.75) and each model was moving at its maximum possible speed while still conforming to the constraint that there be three limbs in contact with the substrate at all times. A similar duty factor is seen in the slow, stable gait used by turtles (Jayes and Alexander, 1980). Figures 6 and 7 present the two types of synthetic trackways, narrow and wide, generated by the two sauropod models (see Table 3). For the sake of brevity, only the first half of each 16 frame step-cycle (frames 0 through 7) is shown. The right manus can be seen to protract in frames 1 through 3 and re-establish contact with the substrate by frame 4. Similarly, the left pes protracts in frames 5 through 7 and returns to the ground by frame 8 (not shown). Both mediolateral and forward translation of the bodies are discernable on all the synthetic trackways by

TABLE 3. Mean limb loadings and standard deviations determined for the two walking sauropod models.

	Brachiosaurus brancai		*Diplodocus carnegii*	
	Wide	Narrow	Narrow	Wide
Mean load per arm	35.4 ± 3.36	35.3 ± 3.30	14.4 ± 4.36	21.4 ± 4.88
Mean load per leg	59.3 ± 2.91	59.4 ± 2.99	76.0 ± 9.00	70.2 ± 7.53

Sub-column headings 'Wide' and 'Narrow' refer to the trackway gauges. Loads are averaged over the stance phases of the step cycle, and are expressed as percentages of total body weight.

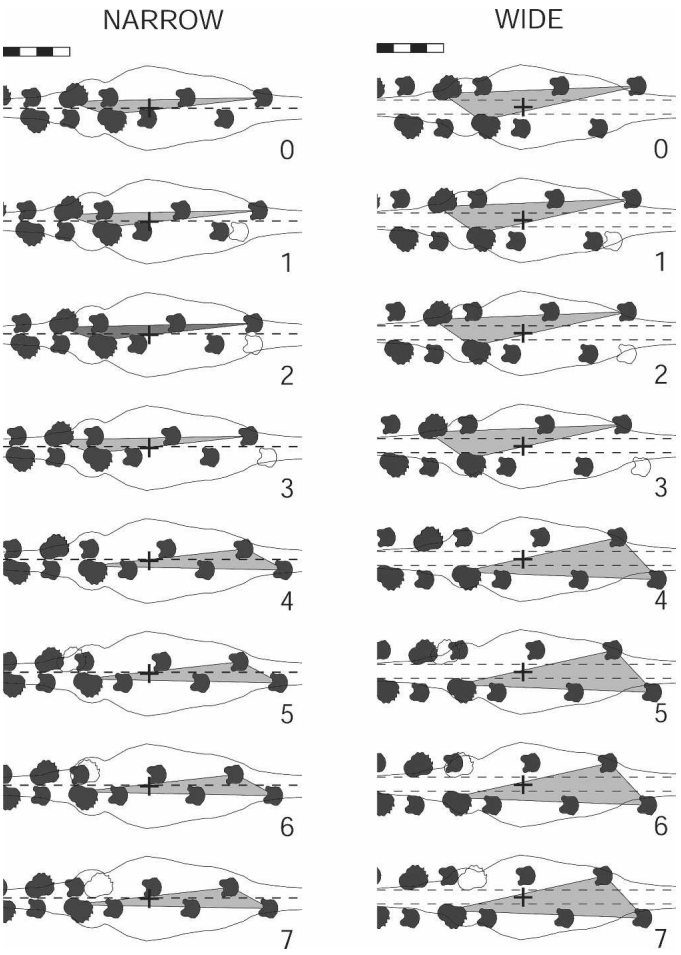

FIGURE 6. Trackway generation and dynamic stability triangles produced by the *Brachiosaurus* model. Medium gray triangles highlight the stability regions defined by three supporting limbs. The larger stability triangle associated with the wide-gauge trackway results in a much more stable model and is the preferred gait for *Brachiosaurus*. Images show just the first 8 frames from a 16 stage walk cycle. On both sets of images frames 1–4 show the right hands (small outlines) protracting, while frames 5–7 show the left feet protracting (large outlines). The rightmost set of dark manus and pes shapes (2 manus + 1 pes, or 1 manus + 2 pedes) on a trackway indicate those limbs that are currently in stance mode, while those footprint shapes towards the left record the tracks made by earlier stance phases. Overlain on each frame is the outline of the trunk and proximal tail (in dorsal view) of the track-making model. The dashed lines along the middle of the trackways mark the lateral margins of the space between the left and right sets of tracks. The black '+' denotes the position of the center of mass of each model. Scale bars are 2 m. Parameters of the trackways and the models are summarized in Tables 2 and 3.

Downloaded From: https://complete.bioone.org/journals/Journal-of-Vertebrate-Paleontology on 21 Mar 2025
Terms of Use: https://complete.bioone.org/terms-of-use

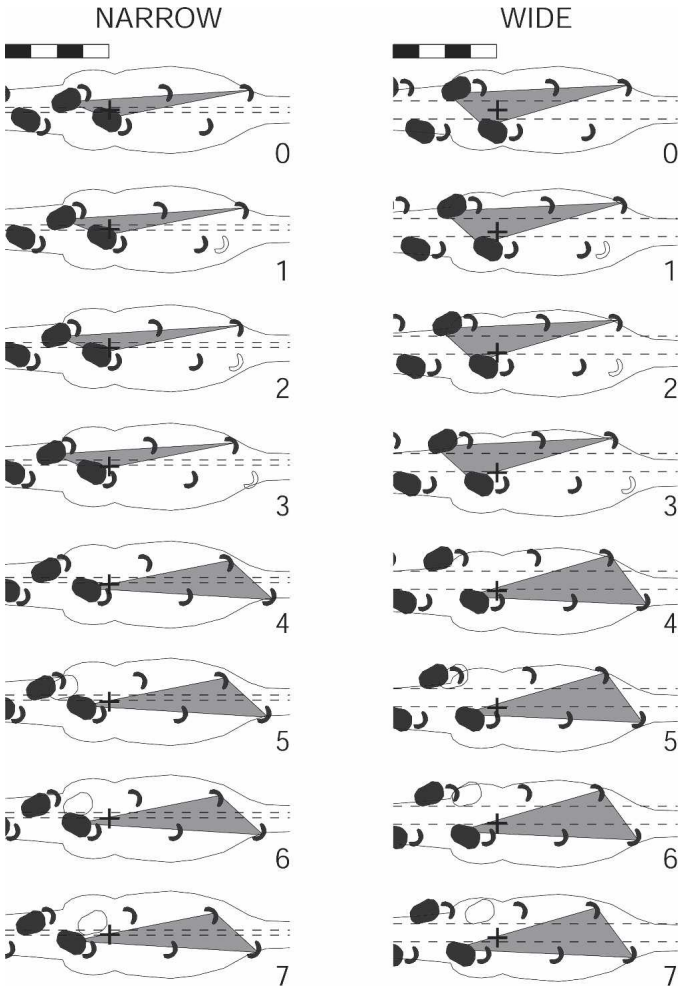

FIGURE 7. Trackway generation and dynamic stability triangles produced by the *Diplodocus* model. The pattern of 'protraction frames' and symbols are the same as that for Figure 6. Despite having a narrow stability triangle during its narrow-gauge mode, the more posteriorly positioned CM of *Diplodocus* remains within the triangle at all times, so this model is stable. The narrow-gauge model of *Diplodocus* has a larger amplitude of mediolateral oscillation (8 cm) than does wide-gauge model *Brachiosaurus*. When the *Diplodocus* model is forced to generate a wide-gauge trackway the model had to oscillate mediolaterally with an amplitude of at least 14 cm just to maintain stability for part of a walk cycle. This mediolateral oscillation of the body is very obvious in the dorsal view, and despite this extra side-to-side motion the model cannot remain stable at all times.

noting the changing position of the widest part of the trunk relative to the dark footprints, although the amount of mediolateral displacement is relatively slight for the *Brachiosaurus* model.

The wide-gauge trackway produced by the *Brachiosaurus* model (right hand side of Fig. 6) represents a plausible replication of *Brontopodus birdi*. The CM remains within the stability triangle at all times, but is very close to the diagonal connecting the contralateral hand-foot pair that form two of the vertices of the triangle. This diagonal line represents the boundary between the current stability region and the next one in the walk sequence, and the stability triangle can be seen to shift forward to its next configuration at frame 4 as the right hand establishes contact with the substrate. As the CM is positioned within the triangle at this stage, the model would be stable when supported by the two hands and the right foot, and it is possible for the left foot to lift off and begin protracting in frames 4 and 5. In this wide-gauge mode, the model of *Brachiosaurus* had the freedom to oscillate mediolaterally up to 20 cm and remain either perfectly stable, or tip slightly forward in the direction of progres-

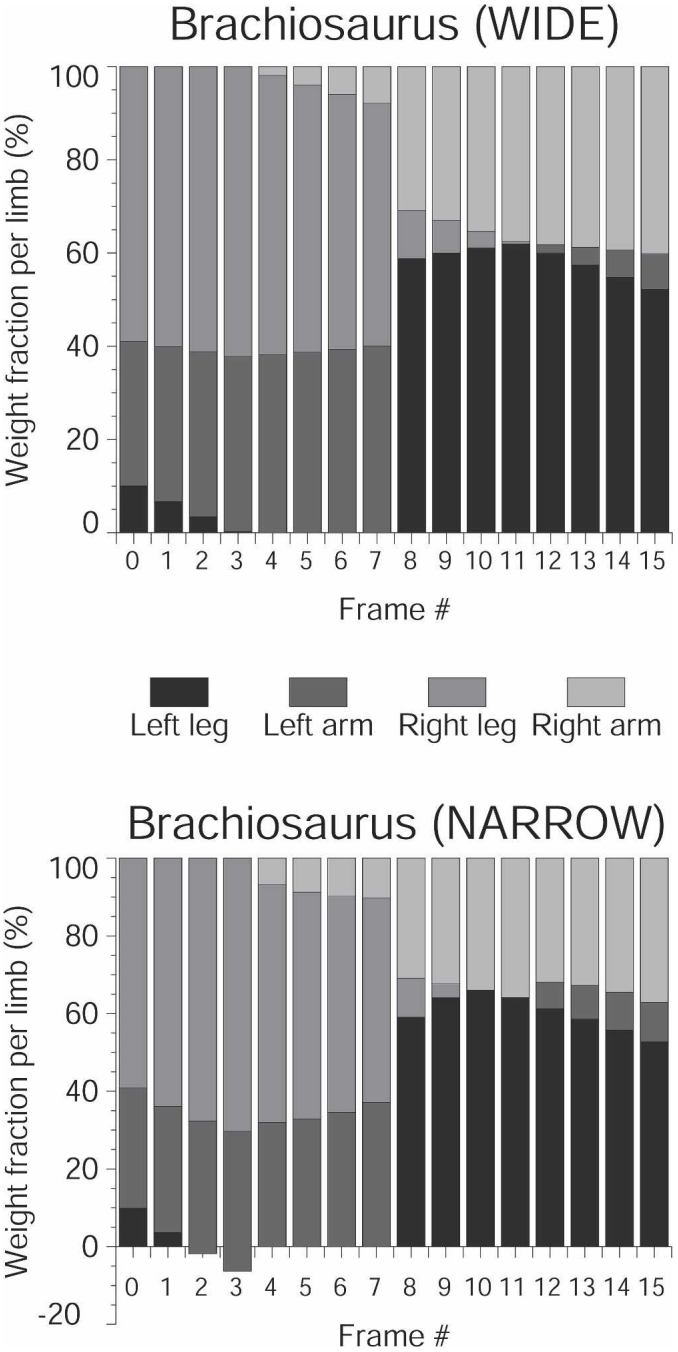

FIGURE 8. Graphical views of the percentage of body weight carried by each *Brachiosaurus* limb at each stage of the narrow- and wide-gauge walk cycles illustrated in Figure 6. Each column of these plots contains the relative fractions of body weight born by all four limbs, and the combined result of all four limbs at each stage sums to 100% of the body weight. Summaries of the loadings are summarized in Table 3. The upper graph shows that when making the wide-gauge trackway all the loads on the limbs are positive and the model will not tip. The lower graph highlights the occurrence of periods of negative loading (Frame 3) during the attempt at producing a narrow-gauge trackway, which indicates that the model was unstable and starting to tip. As predicted by its more anteriorly placed CM, *Brachiosaurus* carries a greater fraction of its weight on its forelimbs than does *Diplodocus* (Fig. 9).

Downloaded From: https://complete.bioone.org/journals/Journal-of-Vertebrate-Paleontology on 21 Mar 2025
Terms of Use: https://complete.bioone.org/terms-of-use

sion. With the lateral displacement set to more than 20 cm, the model would have fallen sideways, because there was no limb in a position to prevent the body from tipping over. These modeling results support the idea of an animal similar to *Brachiosaurus* as a maker of this type of wide-gauge trackway (Farlow et al., 1989; Langston, 1974).

Figure 8 presents the computed loads acting on the limbs of the *Brachiosaurus* model as it was used to generate the two different trackway gauges. The upper graph shows the relatively smoothly varying loads experienced by a leg as it was in the stance phase for 12 frames in succession (8 through 15, 0 through 3). The loads on the legs can be seen to increase for the first 3 or 4 frames of the stance phase, attain their maximum load at midpoint, and then decrease to slightly below their initial load over the 4 frames of the stance action. After eight frames of the stance mode, the leg experiences an abrupt drop in the fraction of body weight that it bears when the support changes from one leg to another. The arms experience simultaneously abrupt increases in loads at these times. These abrupt changes can be seen at the transition between frames 7 and 8, and again between frames 15 and 0 when the cycle begins to repeat itself (Fig. 8). As predicted by the loading equations, the loads experienced by the limbs are always positive when the *Brachiosaurus* model is performing a wide-gauge walk. This model is stable at all stages and the mean fractions of body weight experienced by the forelimbs and hindlimbs are similar to their relative areas (Table 4).

Positioning the *Brachiosaurus* model with its limbs close to the midline replicates a narrow-gauge trackway (left side of Fig. 6). The limbs were repositioned by rotating all the limbs mediad about their proximal ends, and minor changes were made in the stride length and gait angle in an attempt to obtain a stable model when in this narrow-gauge configuration. The CM can be seen to be just inside the triangle for the first three frames, but moves outside the triangle at frame 3. Had this been an actual physical model, it would have tipped laterally to the right at this point as there is no limb projecting laterally on the right side to brace the body. At frame 4, the CM is just barely inside the triangle again due to the generation of a new triangle, and had this been a living animal there would very little margin for error in placing the feet in the correct position to form a valid stability triangle. If the CM were positioned just slightly behind the diagonal of the stability triangle in frame 4, the animal would have tipped to the left and backward. With the limbs of this model brought close to the midline, the area of the stability triangle has shrunk dramatically, and the model is performing the equivalent of 'walking a tightrope' as the amount of lateral motion is limited to no more than 4 cm before left or right sideways tipping would begin.

The *Brachiosaurus* loading pattern is quite different when the model is forced to produce a narrow-gauge trackway (Fig. 8, lower). The loading and unloading patterns are more stepped (i.e., not quite as smooth as is seen for the wide-gauge case), and at least one instance of negative loading is experienced by the left leg and the left arm at frames 2 and 3. Negative loading implies that the animal would have had to grip the substrate and pull itself down to counter a tipping motion. The elephantine hands and feet of a sauropod do not appear to have been well equipped to perform such a function. It is because of the tendency to tip, and the very narrow safety margin, that a narrow-gauge gait for *Brachiosaurus* is rejected.

The left side of Figure 7 shows the *Diplodocus* model generating a narrow-gauge trackway. The posteriorly positioned CM of *Diplodocus* is farther from the hand-foot diagonal, and it is necessary for the body to oscillate mediolaterally with an amplitude of at least 8 cm to maintain the minimum duty factor and to avoid tipping sideways. In this narrow-gauge trackway, the medially positioned feet and more laterally positioned hands have the effect of increasing the obliquity of the hand-foot diagonal, thus shortening the distance between this line and the CM, and minimizing the amount of lateral displacement needed to maintain stability. The upper loading plot of Figure 9 for the narrow-gauge *Diplodocus* confirms that the loads experienced by the limbs of the model are all positive, so this model is stable and would not tip. Additionally, the mean fractions of the body weight experienced by the hands and feet are similar to their relative areas (Table 4).

The right side of Figure 8 has the *Diplodocus* model producing a wide-gauge trackway. Moving the hindfeet of *Diplodocus* into this wide-gauge mode increased the distance of the CM from the diagonal, and required increasing the lateral displacement amplitude to at least 14 cm, which made the model shift rapidly from side-to-side during the walk-cycle. Even with these wider oscillations, the model experienced periods where it was on the verge of tipping backward while protracting a leg. In addition to experiencing negative limb loadings indicative of instability (Fig. 9, lower graph), the relative loadings on the forelimbs of the model exceed by almost a factor of two the relative areas of the handprints, with the hands taking up to 27% of the body weight (frames 7 and 15). For these reasons, *Diplodocus* can be rejected as a potential maker of wide-gauge trackways.

DISCUSSION

With the availability of captive, trained elephants to study it may have been possible to model the walking of elephants to test the reliability of the locomotion simulation software and to make comparisons with sauropod walking. Although this approach was considered, it was rejected for several reasons. The trackways of proboscideans are distinctly different from those of sauropods in that both the footprints and handprints overlap the midline of the trackway, and this is seen in Asian elephants (this study), African elephants (Sikes, 1971), and in tracks attributed to Pleis-

TABLE 4. Summary of body and limb masses, relative CM positions, and density distributions of the 3D body models used in this study.

Taxon	Total mass (kg)	Axial mass (kg)	Leg mass (kg)	Arm mass (kg)	CM*	Thoracic/abdominal density (kg/m^3)	Neck density (kg/m^3)
Elephas maximas	3,089	2,142	235.9	237.5	57.3	950	1,000
Apatosaurus louisae	16,381	13,248	1,271	295	30.4	800	300
Brachiosaurus brancai	25,922	20,716	1,644	954.3	37.4	800	300
Camarasaurus supremus	12,262	10,310	725	250	30.9	800	300
Dicraeosaurus hansemanni	4,349	3,733	260	48	20.9	850	300
Diplodocus carnegii	11,449	9,965	593.6	148.5	11.5	800	300
Haplocanthosaurus priscus	13,564	11,396	918	166	35.4	850	600
Jobaria tiguidensis	22,448	18,764	1,410	422	42.8	850	600
Patagosaurus fariasi	7,888	6,894	347	150	18.0	850	600
Plateosaurus engelhardti	279	231	21	3	11.3	900	600
Shunosaurus lii	2,155	1,706	173	67	27.4	850	600

*Expressed as the percentage of the gleno-acetabular distance in front of the hip socket.

Downloaded From: https://complete.bioone.org/journals/Journal-of-Vertebrate-Paleontology on 21 Mar 2025
Terms of Use: https://complete.bioone.org/terms-of-use

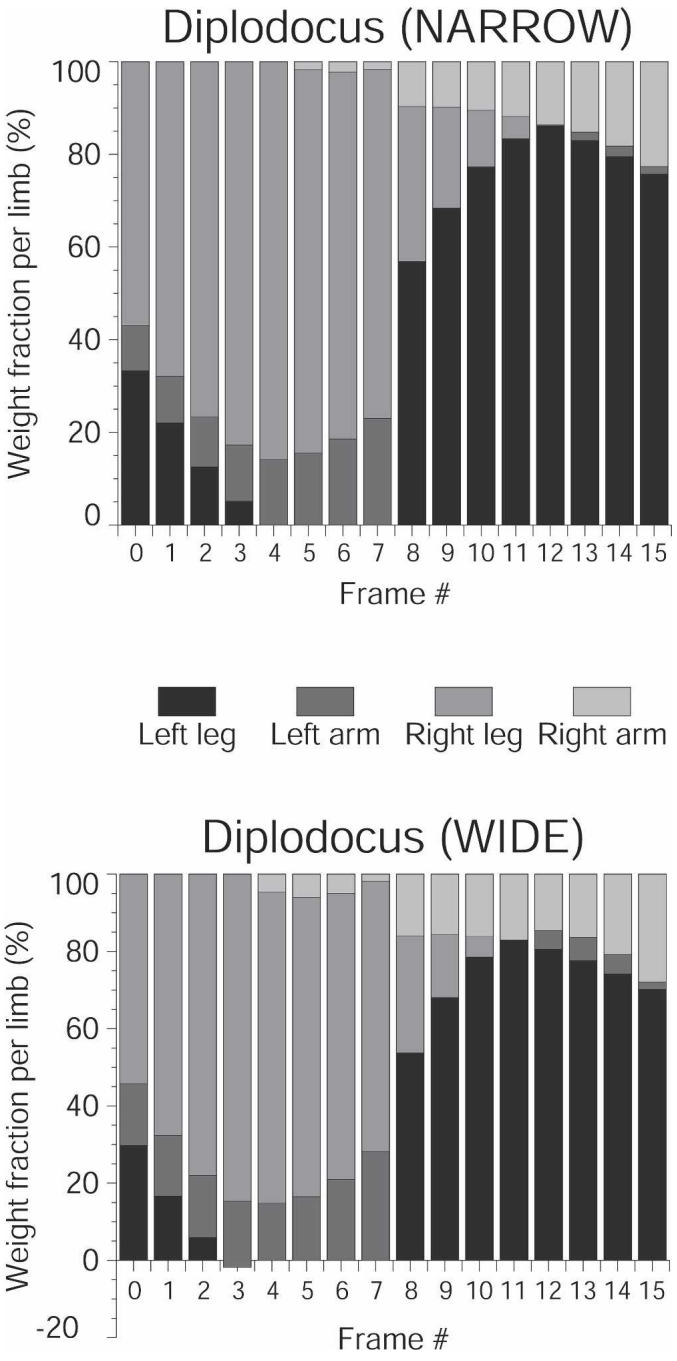

FIGURE 9. Graphical views of the percentage of body weight carried by each *Diplodocus* limb at each stage of the narrow- and wide-gauge walk cycles illustrated in Figure 7. The results of the loadings are summarized in Table 3. The upper graph shows that when making the narrow-gauge trackway all the loads on the limbs are positive and the model will not tip. The lower graph highlights the occurrence of periods of negative loading (Frame 3) during the attempt at producing a wide-gauge trackway, which indicates that the model was unstable and starting to tip. As predicted by its more posteriorly placed CM, *Diplodocus* carries the large majority of its weight on its hindlimbs.

tocene mammoths (McNiel et al., 2005). Moreover, the forelimbs of the elephants carry more of the body weight than the hindlimbs, the opposite of the situation determined for the sauropods. As mammals, elephants are characterized by a mobile, muscle-supported shoulder girdle that contributes to stride length (Hildebrand, 1985), again unlike the situation inferred for dinosaurs (Bennett and Dalzell, 1973). The stride lengths of walking elephants are relatively long (Muybridge, 1887:pl. 110; this study), unlike the relatively short stride lengths inferred for sauropods from their trackways. In addition, the body masses of the Asian elephants of this study range from one third of that calculated for *Diplodocus* to just one eighth of that of *Brachiosaurus*, and this fraction gets smaller when some of the larger titanosaurs are considered. The marked effects of increasing body mass on body support and locomotor potential (Bennett and Dalzell, 1973; Alexander, 1985; Biewener, 1989) make it unreasonable to extrapolate modeling results based on 2.5- to 3.5-ton animals to those weighing 12 ton.

Osteological analysis suggests that strong flexure of the wrist would have been unlikely in sauropods (Christiansen, 1997): in both of the models presented here the wrists were immobilized, but the hands were able to clear the substrate during protraction with just minor flexure at the elbows. Similarly, the only motion in the region of the shoulder girdle was at the glenohumeral joint: no motion of the shoulder girdle relative to the sternal plates was required to produce an effective gait and plausible trackways (contra Paul, 1987; contra Christiansen, 1997). Unexpectedly, the angular excursion of the knee of the *Brachiosaurus* model (44.4º) was observed to be greater than that of *Diplodocus* (33.4º). This can be explained by the crus of *Brachiosaurus* being shorter than the femur, while the crus and femur of *Diplodocus* are less disparate in length. The relatively short shank of *Brachiosaurus* necessitates a larger amount of crural rotation to effect the required length changes associated with flexion and extension of the limb. This greater knee excursion of *Brachiosaurus* is similar to what has been inferred for titanosaurs based on the enlarged articular surfaces of their distal femoral condyles (Wilson and Carrano, 1999). Given the close phylogenetic association between *Brachiosaurus* and titanosaurs (Upchurch et al., 2004) this observation provides another indication of the plausibility of the model.

Published examples of narrow-gauge trackways show that the manus prints are positioned anterolaterally relative to those of the pes (e.g., Fig. 1A – iii and iv). The synthetic, narrow-gauge trackway generated by the *Brachiosaurus* model differs from the typical configuration in that its manus prints are directly in front of those of the pes. This modification was required so that the model started in a state of stable equilibrium. Figure 10 shows the situation when the forelimbs of *Brachiosaurus* were positioned more laterally in an attempt to more accurately mimic a narrow-gauge trackway. The CM ('+' sign) misses the triangle completely so this model doesn't even begin to be stable. The configuration of the limbs in Figure 10 is such that left arm and right leg are at the beginning of protraction, while the left leg has completed two-thirds of its retraction phase. The next limb to be protracted at this point in the gait cycle is the right arm, but it would have been impossible for the model to lift its right arm off of the substrate because there would be a fraction of the body weight acting on this limb. An alternative could be to form a stability triangle composed of the left and right hands and the right foot, and to lift the left leg. However, this would lead to conflicts between the timing and sequence of protractions of the other limbs later in the cycle. A living animal, reacting to an irregular substrate, could deal with this sort of complexity, but for these minimalist sauropod models, a steady, rhythmic gait is the only one considered. Another aspect of actual narrow-gauge trackways is that the manus prints lie immediately anterior to the pes prints. It was not possible to obtain such a configuration and have a stable model with the limbs of the modeled *Brachiosaurus* model.

Titanosaurs dominated Cretaceous sauropod faunas, but their remains are poorly known compared with those of Late Jurassic sauropods (Wilson and Carrano, 1999). The close relationship

Downloaded From: https://complete.bioone.org/journals/Journal-of-Vertebrate-Paleontology on 21 Mar 2025
Terms of Use: https://complete.bioone.org/terms-of-use

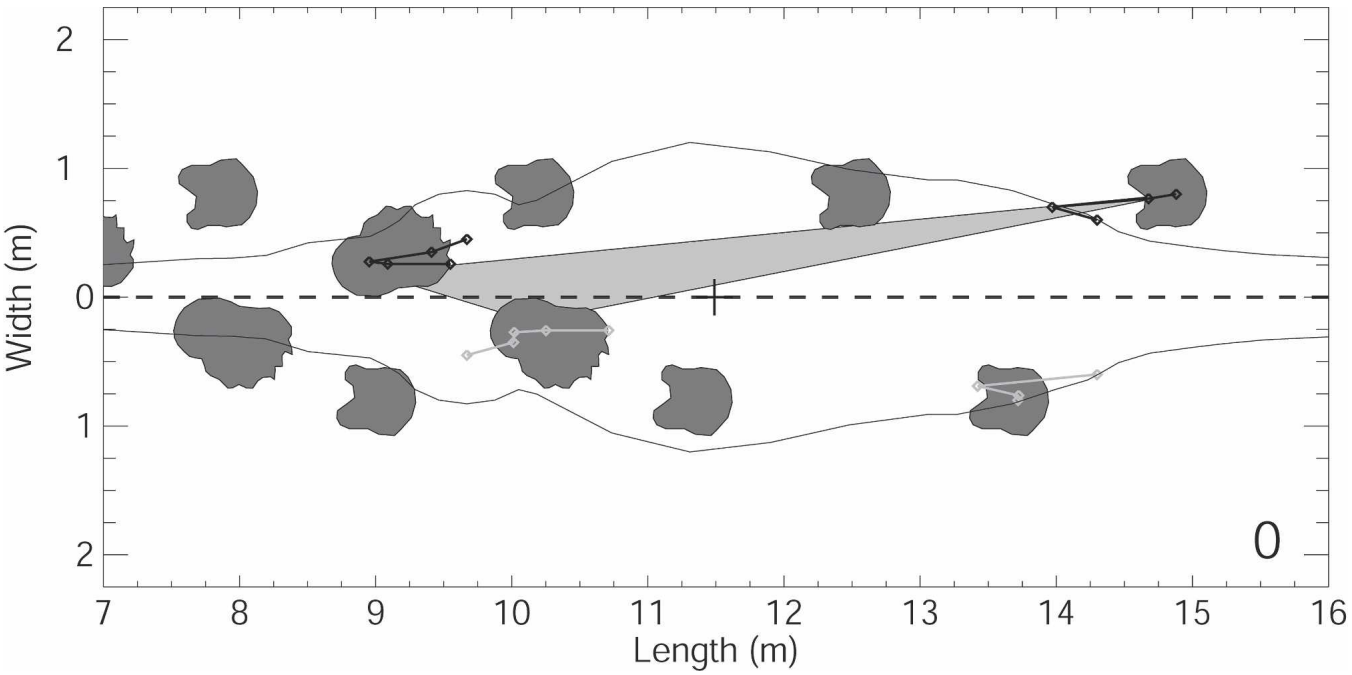

FIGURE 10. An alternate form of narrow-gauge attempted with the *Brachiosaurus* model. Typical narrow-gauge, sauropod trackways have their handprints anterolaterally positioned relative to the footprints, but when this configuration was tried with the *Brachiosaurus* model, the CM was not inside the resulting stability triangle at the very beginning of the cycle. For this reason the more medially positioned hand configuration was used in Figure 6.

inferred for brachiosaurids and titanosaurs, and the abundance of wide-gauge trackways from Cretaceous, suggest that titanosaurs possessed body shapes, CM positions, and gaits similar to those of *Brachiosaurus*. Both *Saltasaurus*, a titanosaur from the Late Cretaceous of South America (Powell, 1992), and *Opisthocoelicaudia* (Borsuk-Bialynicka, 1977) had massively constructed pectoral girdles (Wilson and Carrano, 1999), implying that the forelimbs carried a substantial fraction of the body weight. This inference is consistent with the hypothesis that titanosaurs had a more anteriorly positioned CM. Despite suggestions for possible bipedal posture by titanosaurs (Borsuk-Bialynicka, 1977; Powell, 1992; Wilson and Carrano, 1999), the possession of a brachiosaur-type CM position, and the resulting higher body mass moment acting anterior to the hips, would have made it more difficult for these animals to elevate their trunks and necks relative to their hips. A sauropod like *Diplodocus*, with its CM much closer to its hips, would appear to have a better potential to rise up onto its hind legs (Hatcher, 1901; Bakker, 1978).

Predicting Gaits in Other Sauropods

The modeling results suggest that the two derived sauropods in this study had distinctively different gaits. The question then arises as to the primitive gait for sauropods as a whole. Both narrow- and wide-gauge trackways are known from the Middle Jurassic (Lockley et al., 1994; Day et al., 2002, 2004), and predate the derived Late Jurassic *Diplodocus* and *Brachiosaurus*. With the aim of investigating this question of 'gauge-priority,' an additional seven sauropod body and limb models were generated and their total masses and centers of mass were determined (summarized in Table 2). One prosauropod model, *Plateosaurus*, was also produced to act as an outgroup for Sauropoda, and Figure 11 presents lateral and dorsal views of these models. In constructing these additional models, the assigned density distributions were guided by the degree of pneumaticity inferred for the axial skeleton of each taxon as determined by Wedel (2003b: Table 4). Although there is a virtually complete skeleton of the titanosaur *Rapetosaurus krausei* (Curry Rogers and Forster, 2001), there is no illustration of the animal in dorsal view to enable the generation of a reliable three-dimensional model. For this reason, and the lack sufficient articulated skeletal material for other titanosaurs, these sauropods were excluded from this study.

Plotting the relative position of the CM against body mass for all of the models in this study reveals a trend for larger taxa to have CMs that are more anteriorly positioned (Fig. 12). *Plateosaurus* is the lightest animal of the set, and has the most posteriorly positioned CM, implying that the loads on its forelimbs would have been very low. The two heaviest taxa of this study, *Brachiosaurus* and *Jobaria*, have CMs that are positioned not less than 37% of their GA distance. This pattern of a more forwardly placed CM in heavier forms is repeated independently within the Diplodocoidea where the 16.4-ton *Apatosaurus* has its CM at 30.4 % GA while the 11.5-ton *Diplodocus* has its CM at just 11.5%.

A CM close to the hips is seen in habitually bipedal dinosaurs (Alexander, 1985; Henderson, 1999), and the posterior position for the CM of *Plateosaurus* is consistent with the suggestion that this dinosaur was facultatively bipedal (Van Heerden, 1997). Possible prosauropod trackways have been identified from the Chinle Group of New Mexico (Lockley and Hunt, 1995:fig. 3.13), and two of these trackways (Peacock Canyon) exhibit the typical narrow-gauge form with the pes prints overlapping the trackway midline, and small manus prints positioned immediately anterolaterally to the pes prints. *Plateosaurus* is the most primitive of the taxa included in Figure 12, and its assignment as a potential generator of narrow-gauge trackways suggest that the primitive gauge for sauropods was the narrow one. The two most primitive sauropods known from relatively complete skeletons—*Patagosaurus* and *Shunosaurus* (Fig. 11)—have posteriorly posi-

Downloaded From: https://complete.bioone.org/journals/Journal-of-Vertebrate-Paleontology on 21 Mar 2025
Terms of Use: https://complete.bioone.org/terms-of-use

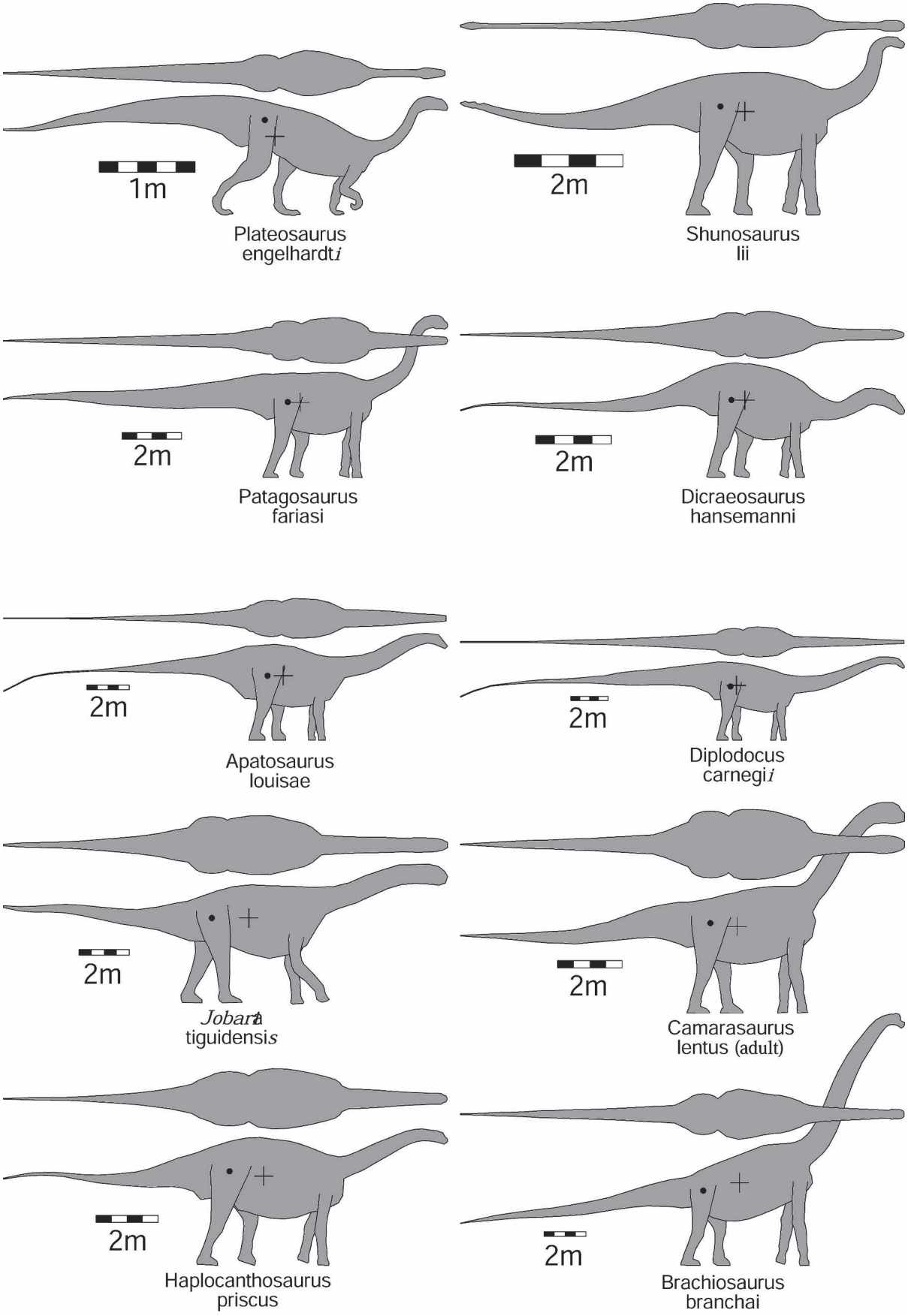

Downloaded From: https://complete.bioone.org/journals/Journal-of-Vertebrate-Paleontology on 21 Mar 2025
Terms of Use: https://complete.bioone.org/terms-of-use

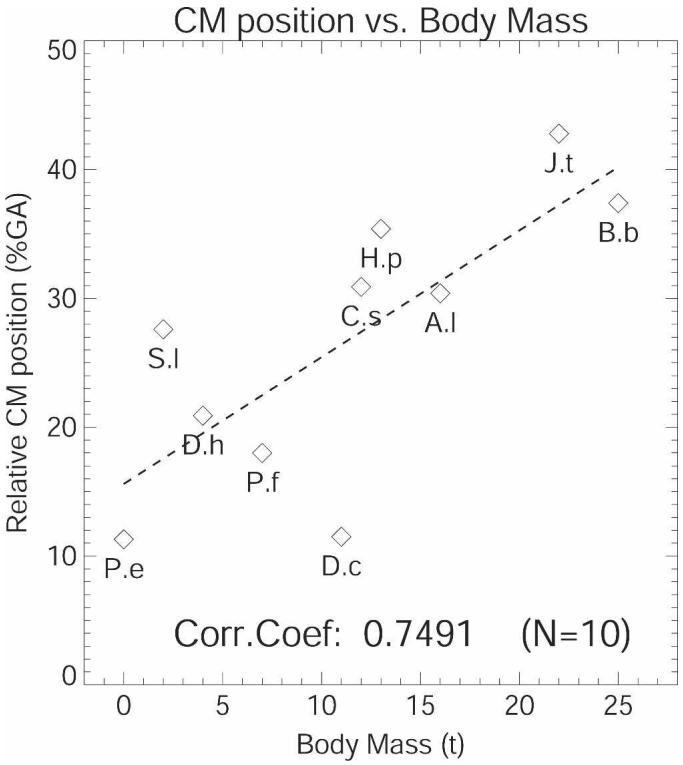

FIGURE 12. Plot showing the positive correlation between body mass in sauropods and a more anteriorly positioned CM, with the CM position expressed as the fraction of the gleno-acetabular (GA) distance that it lies in front of the acetabulum. In light of the problems with the *Brachiosaurus* model and its attempts to walk with a narrow-gauge, it is proposed that all sauropods with CMs positioned at or beyond 30% of the GA distance will be forced to walk with a wide-gauge trackway. Thus *Haplocanthosaurus* (H.p) and *Jobaria* (J.t) will be wide-gauge like *Brachiosaurus* (B.b); *Camarasaurus* (C.s) and *Apatosaurus* (A.l) will be of intermediate gauge; and *Patagosaurus* (P.f), *Shunosaurus* (S.l), and *Dicraeosaurus* (D.h) will be narrow-gauge like *Diplodocus* (D.c). See Table 4 for the values used to construct this plot.

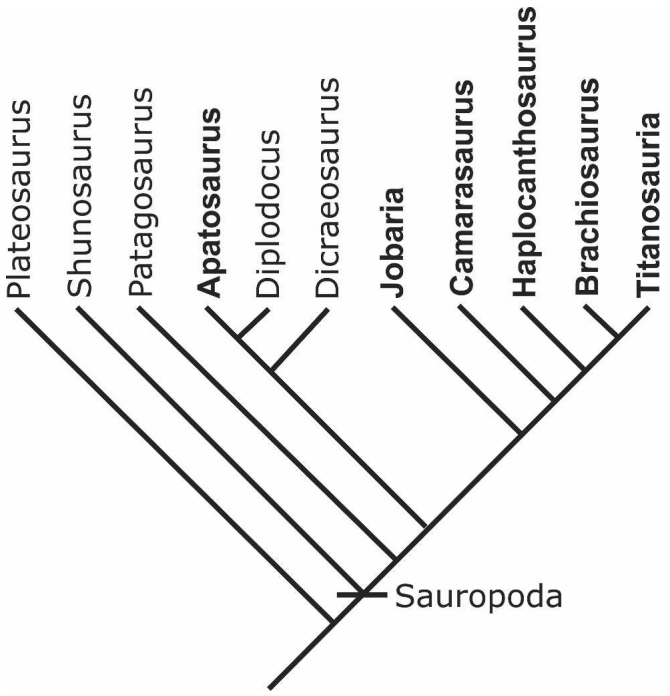

FIGURE 13. Phylogenetic relationships of the taxa in Figure 12 based on the cladogram of Upchurch and colleagues (2004). Those taxa whose names are highlighted in bold have body masses in excess of 12.5 tons and are predicted to have walked with a wide-gauge. This cladogram suggests that narrow-gauge gaits were the primitive state for not only sauropods, but also prosauropods, and that wide-gauge walking sauropods evolved more than once.

tioned CMs (Fig. 12), and like *Diplodocus* they are inferred to have walked with a narrow-gauge gait.

Given that the results of this study demonstrate the incompatibility of a narrow-gauge trackway with an anteriorly positioned CM, the claim is made that all large sauropods (>12 tons) such as *Jobaria*, *Haplocanthosaurus*, and *Camarasaurus* with their more anteriorly positioned CMs would have produced wide-gauge trackways. This prediction is consistent with the proposal that titanosaurs were producing wide-gauge trackways (Wilson and Carrano, 1999), because this sauropod clade includes some of the largest terrestrial animals known to have existed (e.g., *Antarctosaurus* and *Argentinosaurus*: Mazetta et al., 2004). However, this trend does not exclude the possibility that smaller titanosaurids such as *Opisthocoelicaudia* (8.5 t: Paul, 1997) were walking with a wide gait, and the proposed tendency for large sauropods to walk with a wide gauge may be related to overall stability. The more anteriorly positioned CM of the Late Jurassic *Apatosaurus* (Table 2) hints that it may have walked in such a way to create a trackway that had more in common with a wide-gauge one. Trackway (iv) of Figure 1 (also from the Late Jurassic), with its larger manus prints could, therefore, be attributed to something like *Apatosaurus*. This inference is supported by the existence of a possible basal diplodocid in the Middle Jurassic of central England (Upchurch and Martin, 2003), and the presence of relatively narrow 'wide-gauge' tracks from the same region and time period (Day et al., 2004). The trend observed in Figure 12 contradicts the claim of Day et al. (2002, 2004) that trackway gauge is not a function of body size. A cladogram for the set of taxa used in this study (Fig. 13) shows that very large body size evolved more than once within Sauropoda, and it appears that all clades of sauropods had the potential to evolve taxa capable of generating wide-gauge trackways.

CONCLUSIONS

The combination of the negative limb loads, excessive mediolateral motions, and overloading of the hands and forelimbs, leads to the rejection of *Diplodocus* as the generator of wide-gauge trackways. In contrast, the modest mediolateral motions, a loading pattern on the hands and feet consistent with their relative areas, and stability of the narrow-gauge walking *Diplodocus*

←

FIGURE 11. Dorsal and right lateral views of additional sauropod body models used to look for trends in CM position over time. Models were adapted from the following sources: *Brachiosaurus* and *Plateosaurus* (Paul, 1987); *Apatosaurus*, *Camarasaurus*, *Dicraeosaurus*, *Diplodocus*, *Haplocanthosaurus*, *Patagosaurus*, and *Shunosaurus* (Paul, 1997); and *Jobaria* (Sereno et al., 1999). On each model the black dot locates the position of the hip socket, while the black '+' marks the position of center of mass of the body+limbs. See Table 4 for details of component masses and density distributions.

Downloaded From: https://complete.bioone.org/journals/Journal-of-Vertebrate-Paleontology on 21 Mar 2025
Terms of Use: https://complete.bioone.org/terms-of-use

model support the identification of this dinosaur, and other sauropods with posteriorly positioned centers of mass, as makers of narrow-gauge trackways. The stability of the wide-gauge walking *Brachiosaurus* model, and its replication of the ichnogenus *Brontopodus birdi*, suggests that brachiosaurids and other large sauropods with more anteriorly positioned centers of mass, were the makers of wide-gauge trackways. The ability of *Brachiosaurus* to walk with a gait that produces a narrow-gauge trackway is rejected because of a tendency to tip, and the existence of a narrow safety margin. It is proposed that narrow-gauge walking was the primitive trait for sauropods, and that walking with a gait that produced a wide-gauge trackway was a necessity for large (>12.5 ton) sauropods. Given the wide phylogenetic distribution of sauropods interpreted to have walked with a wide gauge, it appears that this habit arose independently within different clades of sauropods.

ACKNOWLEDGMENTS

I thank Eric Snively for the title, constructive criticisms, and suggestions for improvement of the text and figures, and Anthony P. Russell for comments on an earlier version. Both are in the Department of Biological Sciences, University of Calgary. Thanks also to people at Calgary Zoo—keepers Bob Kam, Dave Percival, and Les O'Brian for carrying out the elephant weighings and walkings, Tian Everest for facilitating the zoo work, and Leah Maskewich for assistance. The comments and suggestions of the two reviewers, Jim Farlow and Matt Wedel, improved this paper, as did the editorial efforts of Paul Barrett. This work was supported by a Natural Sciences and Engineering Research Council of Canada post-doctoral fellowship awarded to the author, a University Technologies Inc. Fellowship, and a grant from the Jurassic Foundation.

LITERATURE CITED

Alexander, R. McN. 1985. Mechanics of posture and gait of some large dinosaurs. Zoological Journal of the Linnean Society 83:1–25.

Alexander, R. McN. 1997. Engineering a dinosaur; pp. 414–425 in J. O. Farlow and M. K. Brett-Surman (eds.), The Complete Dinosaur. Indiana University Press, Bloomington.

Bakker, R. T. 1978. Dinosaur feeding behaviour and the origin of flowering plants. Nature 274:661–663.

Bennett, A. F., and B. Dalzell. 1973. Dinosaur physiology: a critique. Evolution 27:170–174.

Biewener, A. A. 1989. Scaling body support in mammals: limb posture and muscle mechanics. Science 245:45–48.

Bonnan, M. F. 2003. The evolution of manus shape in sauropod dinosaurs: implications for functional morphology, forelimb orientation, and phylogeny. Journal of Vertebrate Paleontology 23:595–613.

Borsuk-Bialynicka, M. A. 1977. A new camarasaurid sauropod *Opisthocoelicaudia skarzynkskii*, gen. n. sp. n. from the Upper Cretaceous of Mongolia. Palaeontologica Polonica 37:45–64.

Bramwell, C. B., and G. R. Whitfield. 1974. Biomechanics of *Pteranodon*. Philosophical Transactions of the Royal Society of London, Series B 267:503–581.

Christian, A., and W.-D. Heinrich. 1998. The neck posture of *Brachiosaurus brancai*. Mitteilungen aus dem Museum für Naturkunde in Berlin. Geowissenschaflicher Reihe 1:73–80.

Christiansen, P. 1997. Locomotion in sauropod dinosaurs. Gaia 14:45–75.

Curry Rogers, K., and C. A. Forster. 2001. The last of the dinosaur titans: a new sauropod from Madagascar. Nature 412:530–534.

Daniels, C. B., and J. Pratt. 1992. Breathing in long necked dinosaurs: did the sauropods have bird lungs? Comparative Biochemistry and Physiology 101A(1):43–46.

Day, J. J., D. B. Norman, A. S. Gale, P. Upchurch, and H. P. Powell. 2004. A Middle Jurassic dinosaur trackway site from Oxfordshire, UK. Palaeontology 47:319–348.

Day, J. J., P. Upchurch, D. B. Norman, A. S. Gale, and H. P. Powell. 2002. Sauropod trackways, evolution, and behaviour. Science 296: 1659.

Dutuit, J.-M., and A. Ouazzou. 1980. Découverte d'une piste de Dinosaure sauropode sur la site d'empreintes de Demnat (Haut-Atlas marocain). Mémoires de la Société Géologique de France, n.s. 139: 195–102.

Farlow, J. O. 1987. A guide to Lower Cretaceous dinosaur footprints and tracksites of the Paluxy River Valley, Somervell County, Texas. Field Trip Guidebook, South-Central Section, Geological Society of America, Baylor University, Waco, Texas, 50 pp.

Farlow, J. O. 1992. Sauropod tracks and trackmakers: integrating the ichnological and skeletal records. Zubia 10:89–138.

Farlow, J. O., J. G. Pittman, and J. M. Hawthorne. 1989. *Brontopodus birdi*, Lower Cretaceous dinosaur footprints from the U.S. Gulf Coast Plain; pp. 371–394 in D. D. Gillette and M. G. Lockley (eds.), Dinosaur tracks and traces. Cambridge University Press, Cambridge.

Gambaryan, P. P. 1974. How Mammals Run. John Wiley and Sons, New York, 367 pp.

Gray, J. 1968. Animal Locomotion. Weidenfeld and Nicolson, London, 479 pp.

Gunga, H.-C., K. A. Kirsch, F. Baartz, and L. Röcker. 1995. New data on the dimensions of *Brachiosaurus brancai* and their physiological implications. Naturwissenchaften 82:190–192.

Halliday, D., R. Resnick, and J. Walker 1993. Fundamentals of Physics, 4th ed. John Wiley and Sons, New York, 977 pp.

Hatcher, J. B. 1901. *Diplodocus* (Marsh): its osteology, taxonomy, and probable habits, with a restoration of the skeleton. Memoirs of the Carnegie Museum 1:1–63.

Henderson, D. M. 1999. Estimating the mass and centers of mass of extinct animals by 3D mathematical slicing. Paleobiology 25:88–106.

Henderson, D. M. 2002. The eyes have it: the sizes, shapes, and orientations of theropod orbits as indicators of skull strength and bite force. Journal of Vertebrate Paleontology 22:766–778.

Henderson, D. M. 2004. Tipsy punters: sauropod dinosaur pneumaticity, buoyancy, and aquatic habits. Proceedings of the Royal Society of London, Series B–Biology Letters 271:S180–S183.

Henderson, D. M. (in press). Forces and stresses in a walking ostrich: a three-dimensional, computational model. Journal of Theoretical Biology.

Hildebrand, M. 1985. Walking and running; pp. 38–57 in M. Hildebrand, D. M. Bramble, K. F. Liem, and D. B. Wake (eds.), Functional Vertebrate Morphology. Harvard University Press, Cambridge.

Ishigaki, S. 1985. Dinosaur footprints of the Atlas Mountains. Nature Study 31:136–139.

Jayes A. S., and R. McN. Alexander. 1980. The gaits of chelonians: walking techniques for very low speeds. Journal of Zoology 191: 353–378.

Langston, W., Jr. 1974. Nonmammalian Comanchean tetrapods. Geosciences and Man 8:77–102.

Lockley, M. G., and A. P. Hunt. 1995. Dinosaur tracks and other fossil footprints of the western United States. Columbia University Press, New York, 338 pp.

Lockley, M. G., J. O. Farlow, and C. A. Meyer. 1994. *Brontopodus* and *Parabrontopodus* ichonogen nov. and the significance of wide- and narrow-gauge sauropod trackways. Gaia 10:135–145.

Mazzetta, G. V., P. Christiansen, and R. A. Farina. 2004. Giants and bizarres: body size of some South American Cretaceous dinosaurs. Historical Biology 16:1–13.

McIntosh, J. S., M. K. Brett-Surman, and J. O. Farlow. 1997. Sauropods; pp. 264–290 in J. O. Farlow and M. K. Brett-Surman (eds.), The Complete Dinosaur. Indiana University Press, Bloomington.

McMahon, T. A. 1975. Allometry and biomechanics: limb bones in adult ungulates. American Naturalist 109:547–563.

McNeil, P., L. V. Hills, B. Kooyman, and S. M. Tolman. 2005. Mammoth tracks indicate a declining Late Pleistocene population in southwestern Alberta, Canada. Quaternary Science Reviews 24:1253–1259.

Muybridge, E. 1887. Animal locomotion. An electrophotographic investigation of consecutive phases of animal movements. Lippincott, Philadelphia, 72 pp.

Paul, G. S. 1987. The science and art of restoring the life appearance of dinosaurs and their relatives: a rigorous how-to guide; pp. 5–49 in S. J. Czerkas and E. C. Olson (eds.), Dinosaurs Past and Present, Vol II. Natural History Museum of Los Angeles County and University of Washington Press, Seattle.

Paul, G. S. 1997. Dinosaur models: the good, the bad, and using them to estimate the mass of dinosaurs; pp. 129–154 in D. L. Wolberg, E.

Downloaded From: https://complete.bioone.org/journals/Journal-of-Vertebrate-Paleontology on 21 Mar 2025
Terms of Use: https://complete.bioone.org/terms-of-use

Stump, and G. D Rosenberg (eds.), Dinofest International Proceedings. Academy of Sciences, Philadelphia.
Pecksis, J. 1994. Implications of body-mass estimates for dinosaurs. Journal of Vertebrate Paleontology 14:520–533.
Pittman, J. G. 1984. Geology of the De Queen Formation of Arkansas. Transactions of the Gulf Coast Association of Geological Societies 34:201–209.
Powell, J. E. 1992. Osteologia de *Saltasaurus loricatus* (Sauropoda-Titanosauridae) del Cretacio Superior del noroeste Argentino; pp. 165–230 in J. L. Sanz and A. D. Buscalioni (eds.), Los Dinosaurios y Su Entorno Biotico. Institutio "Juan de Valdes," Cuenca.
Proctor, N. S., and P. J. Lynch. 1993. Manual of Ornithology. Yale University Press, New Haven, 340 pp.
Robinson, J. R. and E. C. Frederick. 1989. Scaling of foot dimensions. Journal of Biomechanics 22:979–1111.
Schmidt-Nielsen, K. 1984. Scaling: why is animal size so important. Cambridge University Press, Cambridge, 241 pp.
Sereno, P. C., A. L. Beck, D. B. Dutheil, et al. 1999. Cretaceous sauropods from the Sahara, and the uneven rate of skeletal evolution among dinosaurs. Science 286:1342–1347.
Sikes, S. K. 1971. The Natural History of the African Elephant. Weidenfeld and Nicolson, London, 397 pp.
Stahl, W. R. 1967. Scaling of respiratory variables in mammals. Journal of Respiratory Physiology 22:453–460.
Thulborn, T. 1990. Dinosaur Tracks. Chapman and Hall, London, 410 pp.
Upchurch, P., and J. Martin. 2003. The anatomy and taxonomy of *Cetiosaurus* (Saurischia, Sauropoda) from the Middle Jurassic of England. Journal of Vertebrate Paleontology 23:208–231.
Upchurch, P., P. M. Barrett, and P. Dodson. 2004. Sauropoda; pp. 259–322 in D. B. Weishampel, P. Dodson, and H. Osmólska (eds.), The Dinosauria, 2nd Ed. University of California Press, Berkeley.
Van Heerden, J. 1997. Prosauropods; pp. 242–263 in J. O. Farlow and M. K. Brett-Surman (eds.), The Complete Dinosaur. Indiana University Press, Bloomington.
Wedel, M. J. 2003a. Vertebral pneumaticity, air sacs, and the physiology of sauropod dinosaurs. Paleobiology 29:243–255.
Wedel, M. J. 2003b. The evolution of vertebral pneumaticity in sauropod dinosaurs. Journal of Vertebrate Paleontology 23:344–357.
Wedel, M. J. 2004. Skeletal pneumaticity in saurischian dinosaurs and its implications for mass estimates. Journal of Vertebrate Paleontology 24 (3-Suppl.):127A.
Wedel, M. J., and R. L. Cifelli. 2005. *Sauroposeidon*: Oklahoma's native giant. Oklahoma Geology Notes 65:40–57.
Wedel, M. J., R. L. Cifelli, and R. K. Sanders. 2000. Osteology, paleobiology, and relationships of the sauropod dinosaur *Sauroposeidon*. Acta Palaeontologica Polonica 45:343–388.
Wilson, J. A., and M. T. Carrano. 1999. Titanosaurs and the origin of "wide-gauge" trackways: a biomechanical and systematic perspective on sauropod locomotion. Paleobiology 25:252–267.

Submitted 28 November 2005; accepted 24 June 2006.

Downloaded From: https://complete.bioone.org/journals/Journal-of-Vertebrate-Paleontology on 21 Mar 2025
Terms of Use: https://complete.bioone.org/terms-of-use